The calcium sensor synaptotagmin 7 is required for synaptic facilitation

Citation

Published Version

Permanent link

Terms of Use

Share Your Story

The calcium sensor synaptotagmin 7 is required for synaptic facilitation

Skyler L. Jackman[1], **Josef Turecek**[1], **Justine E. Belinsky**[1], and **Wade G. Regehr**[1]

[1]Department of Neurobiology, Harvard Medical School, 220 Longwood Avenue, Boston, Massachusetts 02115, USA

Abstract

It has been known for over 70 years that synaptic strength is dynamically regulated in a use-dependent manner[1]. At synapses with a low initial release probability, closely spaced presynaptic action potentials can result in facilitation, a short-term form of enhancement where each subsequent action potential evokes greater neurotransmitter release[2]. Facilitation can enhance neurotransmitter release manyfold and profoundly influence information transfer across synapses[3], but the underlying mechanism remains a mystery. Among the proposed mechanisms is that a specialized calcium sensor for facilitation transiently increases the probability of release[2,4] and is distinct from the fast sensors that mediate rapid neurotransmitter release. Yet such a sensor has never been identified, and its very existence has been disputed[5,6]. Here we show that synaptotagmin 7 (syt7) is a calcium sensor that is required for facilitation at multiple central synapses. In syt7 knockout mice, facilitation is eliminated even though the initial probability of release and presynaptic residual calcium signals are unaltered. Expression of wild-type syt7 in presynaptic neurons restored facilitation, whereas expression of a mutated syt7 with a calcium-insensitive C2A domain did not. By revealing the role of syt7 in synaptic facilitation, these results resolve a longstanding debate about a widespread form of short-term plasticity, and will enable future studies that may lead to a deeper understanding of the functional importance of facilitation.

Several mechanisms for facilitation have been proposed (Extended Data Fig. 1). In the "buffer saturation" model, high concentrations of presynaptic Ca^{2+} buffer capture incoming Ca^{2+} before it binds to the rapid synaptotagmin isoforms (1, 2 and 9) that trigger vesicle fusion at most synapses[7]. If the Ca^{2+} buffer saturates during the first action potential, more Ca^{2+} reaches release sites during subsequent action potentials, producing facilitation[6,8]. Yet many facilitating synapses lack sufficient presynaptic Ca^{2+} buffer to account for this form of facilitation[9]. Another theory suggests that a specialized Ca^{2+} sensor responds to the smaller,

Correspondence to: Wade G. Regehr.

longer-lasting Ca^{2+} signals between action potentials[4]. Under one scenario, this sensor modulates Ca^{2+} channels to produce use-dependent increases in Ca^{2+} influx[10]. Several candidate proteins have been proposed to act in this manner[11,12], but increased Ca^{2+} influx cannot account for facilitation at most synapses[13]. Alternatively, an unidentified Ca^{2+} sensor could mediate facilitation by directly increasing the probability of release (*p*).

Syt7 is located presynaptically, and binds Ca^{2+} with high affinity and slow kinetics[14–16], making it a promising candidate sensor for the modest increases in residual Ca^{2+} that mediate facilitation. Previous studies suggest that syt7 contributes to a slow phase of transmission known as asynchronous release[17,18], and to Ca^{2+}-dependent recovery from depression[19], but the role of syt7 in facilitation was not examined because these studies employed synapses with prominent depression that obscures facilitation. We therefore examined synaptic transmission at four facilitating synapses: Schaffer collateral synapses between hippocampal CA3 and CA1 pyramidal cells[9] (Fig. 1a), thalamocortical synapses between layer 6 cortical pyramidal cells and thalamic relay cells[20] (Fig. 1b), mossy fiber synapses between dentate granule and CA3 cells[9] (Fig. 1c), and perforant path synapses between layer II/III cells of the entorhinal cortex and dentate granule cells[21] (Fig. 1d). Immunohistochemistry shows that syt7 is present in regions where these synapses are located (Extended Data Figs. 2 and 3). Facilitation is often assessed using pairs of closely-spaced stimuli. In slices from wild-type (WT) mice, paired-pulse facilitation resulted in ~2-fold enhancement of neurotransmitter release lasting several hundred milliseconds (Fig. 1a–d, black traces). In syt7 knockout (KO) mice, paired-pulse facilitation was eliminated (Fig. 1a–d, red traces). Sustained high frequency activation produces up to 10-fold enhancement in wild-type animals, but in knockouts facilitation is eliminated at all synapses except for mossy fiber synapses, where the remaining enhancement is consistent with use-dependent spike broadening that occurs at this synapse[22] (Fig. 1e–h, Extended Data Fig. 4).

The loss of facilitation in syt7 knockouts cannot be accounted for by slowed recovery from depression reported with syt7 deletion[19], because recovery from depression is too slow to strongly influence rapid facilitation, nor can it produce the large *increase* in release associated with facilitation. There are several possible explanations for the loss of facilitation in knockouts: (1) the presynaptic Ca^{2+} signal that induces facilitation could be altered, (2) the probability of release (*p*) for synaptic vesicles could be increased, which by promoting vesicle depletion would indirectly reduce facilitation, or (3) the mechanism for facilitation could be disrupted directly. We assessed these possibilities at the CA3→CA1 synapse.

Action-potential-evoked increases in presynaptic Ca^{2+} consist of a large, brief localized Ca^{2+} signal that activates the low-affinity Ca^{2+} sensor synaptotagmin 1 to trigger neurotransmitter release[23], and a small residual Ca^{2+} signal (Ca_{res}) that persists for tens of milliseconds and has been implicated in facilitation[2]. It is difficult to measure local Ca^{2+} signals that trigger release, but Ca_{res} is readily measured. We used a low-affinity Ca^{2+} indicator to measure the time course of Ca_{res} in CA3 presynaptic terminals, because facilitation can be attenuated by the accelerated decay of Ca_{res}[4]. Ca_{res} decayed similarly in wild-type and syt7 knockout animals (Fig. 2a), indicating that the loss of facilitation in knockouts is not a consequence of accelerated Ca_{res} decay. We also used Ca_{res} as a measure

of Ca_{influx} to determine whether there are use-dependent manner changes in Ca^{2+} entry. However, each of two closely spaced stimuli evoked the same incremental increase in Ca_{res} in both wild-types and knockouts (Fig. 2b), indicating that use-dependent changes in total Ca_{influx} cannot account for facilitation. This suggests that if changes in Ca_{influx} contribute to facilitation at this synapse, they must be restricted to the small subset of presynaptic calcium channels that evoke neurotransmitter release. We repeated the experiment using a high-affinity Ca^{2+} indicator, where the degree of saturation during paired stimuli can be used to measure the magnitude of Ca_{res} evoked by the first stimulus (see Methods). We conclude that Ca_{influx} evoked by the first stimulus is the same in wild-type and knockout animals (Fig. 2c).

We further explored the role of Ca^{2+} in facilitation by examining the Ca^{2+}-dependence of excitatory postsynaptic currents (EPSC) and facilitation. Raising extracellular Ca^{2+} leads to a steep increase in EPSC amplitude (Fig. 2d), but a decrease in facilitation (Fig. 2e, *black traces*) even though high extracellular Ca^{2+} should *increase* the Ca_{res} available to evoke facilitation. This paradox is resolved by realizing that increased Ca^{2+} influx elevates p, which depletes presynaptic vesicles, saturates release, and limits the extent of facilitation. The Ca^{2+}-dependence of EPSC amplitudes was unaffected in knockout animals (Fig. 2d), but facilitation was absent for all values of external Ca^{2+} (Fig. 2e.f). Meanwhile there was no difference in basal release properties measured by the rate of spontaneous EPSCs (Extended Data Fig. 5). These findings suggest that the loss of facilitation in knockouts is not a consequence of higher initial p, because facilitation was absent even when the initial p was strongly attenuated by reducing external Ca^{2+}.

To further test whether initial p is elevated in syt7 knockouts, we measured how field excitatory postsynaptic potentials (fEPSPs) scaled with stimulus intensity[24] (Fig. 3a). The slope of the fEPSP vs. presynaptic volley gives a relative measure of p (see Methods), which was unchanged in knockouts (Fig. 3b). Moreover, the fEPSP to presynaptic volley ratio changed steeply with extracellular Ca^{2+}, showing that this method is sensitive to p (Fig. 3c, d). We also assessed p using pharmacological blockade of synaptically-activated NMDARs by the use-dependent blocker MK801[25] (Fig. 3e–g). This approach is widely-used to detect changes in p: An increase in p leads to more glutamate release, more activation of NMDARs, and a more rapid blockade of NMDA receptors, while a decrease in p leads to a slower blockade (Extended Data Fig. 6). The rate of blockade of NMDA-mediated field EPSPs (NMDA-fEPSP) was unaffected by syt7 deletion (Fig. 3e), indicating similar initial p. However, when we evoked NMDA-fEPSPs with trains of 3 stimuli[25], amplitudes decayed more rapidly in wild-types (Fig. 3f, g), suggesting that syt7 is required to increase p for the second and third stimuli. Thus, initial p and presynaptic Ca^{2+} signaling are unaffected by syt7 deletion, but knockouts lack the use-dependent increase in p that underlies facilitation. This suggests that the mechanism underlying facilitation is directly impaired by syt7 deletion.

Syt7 is implicated in neuroendocrine release[16], insulin secretion[26], and exocytosis of lysosomes[27], which could all indirectly influence synaptic transmission in global syt7 knockouts. Therefore, to determine whether syt7 controls facilitation by acting in presynaptic neurons in a cell autonomous manner, we tested whether viral expression of syt7

in CA3 pyramidal cells of syt7 knockouts rescued facilitation. This approach is complicated by our inability to virally transduce all CA3 pyramidal cells, which prohibits the use of extracellular stimulation that would activate some presynaptic cells that express syt7 and others that do not. We overcame this problem with an adeno-associated virus (AAV) that drove bicistronic expression of both ChR2 and syt7, allowing optical stimulation of only those fibers expressing syt7.

Using conditions we have previously shown allow facilitation to be studied with optogenetic stimulation (see Methods), we confirmed that when ChR2 alone was expressed, optical and electrical stimulation produced similar facilitation in wild-types (Fig. 4a,e,f), and similar depression in knockouts (Fig. 4b,e,f). We next used a bicistronic vector to express both ChR2 and wild-type syt7 in knockout animals. Light-evoked responses exhibited facilitation, whereas electrically-evoked responses did not (Fig. 4c,e,f). This suggests that bicistronic expression of ChR2 along with a presynaptic protein of interest offers a powerful new approach to characterize the effect of gene manipulation on presynaptic function within intact neural circuits. When syt7 was expressed in wild-type animals the peak facilitation was unaffected (Fig. 4e,f, Extended Data Fig. 7a). Thus, expressing syt7 in CA3 pyramidal cells rescued facilitation in a cell autonomous manner, with facilitation restored only at synapses expressing syt7 and ChR2.

To determine whether Ca^{2+}-binding by syt7 is important for facilitation, we assessed whether facilitation is rescued by syt7 with a mutated Ca^{2+}-insensitive C2A domain (syt7 C2A*). Previous studies established that Ca^{2+}-binding to the C2A domain of syt7 is required for syt7 to mediate asynchronous release[18]. We found that syt7 C2A* did not rescue facilitation in knockouts (Fig. 4d–f). Moreover, in wild-type animals, syt7 C2A* expression strongly attenuated facilitation (Fig. 4e,f, Extended Data Fig. 7b), suggesting that syt7 C2A* competes with native syt7 to suppress facilitation.

Our results indicate that facilitation requires Ca^{2+}-binding to the C2A domain of syt7, and also provide insight into the role of syt7 in facilitation. We conclude that syt7 does not produce facilitation by altering the amplitude and time course of Ca_{res} (Fig. 2), by increasing initial p (Fig. 3), by acting as a Ca^{2+} buffer (Extended Data Fig. 8), or through use-dependent increases in the total Ca_{influx} (Extended Data Fig. 1b, Fig. 2). The observation that initial p is unaltered in syt7 knockouts indicates that local Ca_{influx}, is unaffected for the first stimulus, but it is difficult to rule out the possibility that syt7 mediates a use-dependent increase in Ca_{influx} through the subset of channels that trigger vesicle fusion. There is, however, no evidence for syt7 associating with or regulating calcium channels. In contrast, syt7 is known to interact with syt1 and can mediate vesicle fusion[16–18]. The most parsimonious explanation is that syt7 acts as the hypothesized specialized Ca^{2+} sensor to elevate p during facilitation. Facilitated release exhibits rapid kinetics, suggesting that syt7 somehow increases the probability of syt1-dependent vesicle fusion. Whether this is through a direct interaction of syt7 with a fast synaptotagmin isoform such as syt1 remains an open question. It is also unclear whether the recently described interaction between syt7 and calmodulin that promotes vesicle replenishment[19] is similarly required for facilitation. Finally, it is possible that at other synapses facilitation is mediated by additional specialized

Ca^{2+} sensors or involves other mechanisms. Further studies are needed to clarify these issues.

Based primarily on theoretical considerations, facilitation is thought to profoundly influence both information transfer and network dynamics. In the hippocampus, the high-pass filtering imposed by facilitating synapses may account for the burst firing in place cells that encode spatial information[28]. In the auditory pathway, facilitation is proposed to counteract short-term depression in order to maintain linear transmission of rate-coded sound intensity[29]. It has even been suggested that facilitation forms the basis of short-term memory, as facilitating recurrent connections within cortical networks could support the persistent activity states associated with working memory[30]. In future studies the selective elimination of syt7 from specific cell types could allow the first direct tests of the impact of facilitation on neural circuits and behavior.

Methods

Animals and viruses

All mice were handled in accordance with NIH guidelines and protocols approved by Harvard Medical School. Syt7 KO mice[31] (Jackson Laboratory) and WT littermates of either sex were used. Statistical tests were not used to predetermine sample size. Blinding and randomization were not performed. AAV2/9-hSyn-hChR2(H134R)-EYFP and its pAAV backbone (Addgene 26973) were obtained from the University of Pennsylvania Vector Core. cDNA encoding the rat syt7 WT α isoform and C2A* mutant (D225A, D227A, D233A)[18] were generously provided by Taulant Bacaj and Thomas Sudhof. For rescue experiments involving syt7 with mutated Ca^{2+} binding domains, we used the mutated C2A* version instead of the C2A*C2B* double mutant, as mutation of both C2 domains leads to lower levels of expression. The porcine teschovirus-1 2A (P2A) cleavage sequence[32] and syt7 were inserted after the ChR2 C-terminus in the pAAV backbone (Genscript). Plasmid-driven expression of ChR2-YFP and syt7 was confirmed in HEK cells by syt7 immunostaining and patch-clamp recording of ChR2 photocurrents. AAVs were produced and purified from HEK cells as previously described[33].

Stereotaxic surgeries were performed as described[34]. P18-P30 mice were anesthetized with ketamine/xylazine/acepromazine (100/10/3 mg/kg) supplemented with 1–4% isoflurane. Viruses were injected through glass capillary needles using a syringe (Hamilton) mounted on a stereotaxic instrument (Kopf). Injection coordinates from lambda were 2.69 mm (rostral), 3 mm (lateral), and 2.8 mm (ventral). 1 μl of virus suspension was delivered at a rate of 0.1 μl/min using a a microsyringe pump (WPI; UMP3) and microsyringe pump controller (WPI; Micro4). The needle was slowly retracted 5–10 minutes after injection, and the scalp incision was closed with gluture. Post-injection analgesic (buprenophrine, 0.05 mg/kg) was administered subcutaneously for 48 hrs.

Acute slice preparation

P30-P60 animals were euthanized under isoflurane anesthesia, 14–30 days after AAV injection. Brains were removed and placed in ice-cold solution containing (in mM): 234

sucrose, 25 NaHCO$_3$, 11 glucose, 7 MgCl$_2$, 2.5 KCl, 1.25 NaH$_2$PO$_4$, and 0.5 CaCl$_2$. 270 μm-thick transverse slices (hippocampal recordings) or 250 μm-thick sagittal slices (thalamic recordings) were prepared on a vibratome (Leica, VT1000s), and a cut was made between CA3 and CA1 to prevent recurrent excitation. Slices were transferred for 30 min to 32°C artificial cerebrospinal solution (ACSF) containing (in mM): 125 NaCl, 26 NaHCO$_3$, 25 glucose, 2.5 KCl, 2 CaCl$_2$, 1.25 NaH2PO$_4$, and 1 MgCl$_2$, adjusted to 315 mOsm, and allowed to equilibrate to room temperature for >30 min. Experiments were performed at 33 ± 1°C with flow rates of 2 ml/min.

Electrophysiology

For ChR2 stimulation, 160 mW/mm^2 laser pulses (0.2–0.5 ms) from a 100 mW 473 nm laser (OptoEngine, MBL-III) were focused through the 60X objective of the microscope (Olympus, BX51WI) to produce a 80 μm diameter spot over the stratum radiatum, >500 μm from the recorded cell to avoid activating ChR2 in presynaptic boutons, which can artificially raise the probability of release and obscure facilitation[34]. Extracellular stimulation was performed with a stimulus isolation unit (WPI, A360) using glass monopolar electrodes (0.5–1 MΩ) filled with ACSF. Stimulus electrodes were positioned ~500 μm from the recording electrode in the stratum radiatum (Schaffer collaterals), the internal capsule (corticothalamic), the hillus adjacent to the dentate granule cell layer (mossy fibers), and the outer molecular layer (lateral performant path). To ensure that mossy fiber responses were not contaminated by associational/commissural inputs the metabotropic glutamate receptor agonist DCG-IV (1 μM) was applied at the end of experiments to selectively block mossy fiber responses[35]. Data were included only if responses were reduced by more than 80% (average reduction was 88 ± 1 % in WT and 90 ± 2% in syt7 KO mice), and the amplitude of mossy fiber responses was measured after subtracting the response remaining in the presence of DCG-VI. Stimulus trials were repeated at 0.1 Hz (0.033 Hz at mossy fibers to avoid potentiation), and artifacts were deleted for display. Recordings were acquired using an amplifier (Axon Instruments, Multiclamp 700B) controlled by custom software written in IgorPro (provided by Matthew Xu-Friedman, SUNY Buffalo), and low-pass filtered at 2 kHz. Whole-cell recordings were obtained using borosilicate patch pipettes (2–5 MΩ) pulled with a horizontal puller (Sutter P-97). The internal recording solution contained (in mM): 150 Cs-gluconate, 3 KCl, 10 HEPES, 0.5 EGTA, 3 MgATP, 0.5 NaGTP, 5 phosphocreatine-tris, and 5 phosphocreatine-Na. pH = 7.2. Cells were held at −70 mV, and series resistance was monitored during recordings. fEPSPs were recorded in current-clamp mode with ACSF-filled patch pipettes (0.5–1 MΩ). Inhibition was blocked with picrotoxin (50 μM), and during fEPSP recordings, CPP (2 μM) and CGP (3 μM) was added to the bath. 4–10 trials were conducted for each stimulus frequency, and recordings were averaged over trials. Data in all figures represent the mean ± SEM. Average responses are displayed with double exponential or polynomial curves fit in IgorPro. Unless stated otherwise, statistical significance was assessed by unpaired two-tailed Student's t-test, or one-way ANOVA followed by Tukey's post hoc test.

Probability of release

To record NMDA-EPSCs cells were voltage clamped at +40 mV, and the internal solution contained (in mM): 85 Cs-methanesulfonate, 4 NaCl, 10 HEPES, 0.2 EGTA, 30 BAPTA, 2

MgATP, 0.4 NaGTP, 10 phosphocreatine-Na, 25 TEA, 5 QX-314, pH = 7.3. For recording NMDA-fEPSPs, Mg^{2+} was excluded from ACSF to relieve Mg^{2+} block of NMDA receptors. Picrotoxin (100 μM) and NBQX (5 μM) were added to the bath, and stimulation was conducted at 0.1 Hz (unless otherwise indicated) for 5 minutes to obtain a baseline response. Stimulation was halted for 10 minutes while (+)-MK801 (40 μM) was added and allowed to equilibrate. For experiments involving fEPSPs vs. presynaptic volley, the postsynaptic response was measured by the slope of the fEPSP, while the amplitude of the presynaptic volley was used to determine the number of activated fibers. If p increases, the same number of activated presynaptic fibers will produce a larger fEPSP. The ratio between fEPSP and volley was determined by line fits to the linear regime of the input-output curve of individual experiments (20–80 μA stimuli).

The study of probability of release is complicated because many people use p to refer to the probability of release of a vesicle (p_v) and others refer to probability of release from an active zone ($p_{synapse}$) that contains N vesicles in its readily releasable pool (RRP). Thus, an increase in the size of the RRP for an active zone can increase $p_{synapse}$ even if p_v is unaltered. Although MK801 blockade[25] and fEPSPs vs. presynaptic volley[24] are both widely-used methods to detect changes in the probability of release, for both approaches it is conceivable (though unlikely) that increases in p_v could be obscured by a perfectly balanced decrease in the RRP size. However, the relationship between EPSC amplitude and extracellular Ca^{2+} is similar in WT and syt7 KO animals. This suggests there is no increase in p_v, which would cause this curve to saturate at lower values of Ca_e for syt7 KO animals. Moreover, the large differences in facilitation in WT and syt7 KO animals were even more pronounced when the probability of release was reduced 10-fold by lowering Ca_e from 2 mM to 0.5 mM, which is incompatible with an increase in p_v obscuring facilitation by depleting vesicles.

Ca^{2+} measurements

Ca^{2+} was measured as described previously[4]. Briefly, CA3 fibers were labelled for three minutes using an ACSF-filled pipette containing either magnesium green AM or fura-2 AM (240 μM) and 1% fast green, placed into the border of the CA3-CA1 field. A vacuum pipette placed above the loading site removed excess indicator. Slices were incubated for at least 1 hour and imaging was performed in stratum radiatum of CA1 at least 500 μm from the injection site using a 60X objective and custom-built photodiode. Excitation was achieved using a tungsten (magnesium green) or xenon lamp (fura-2). Schaffer collaterals were stimulated using a glass electrode placed at least 300 μm from the imaging site. To prevent recurrent excitation, experiments were performed in the presence of NBQX (10 μM), CPP (2 μM) and picrotoxin (50 μM).

Magnesium green is a low-affinity calcium indicator[36] (K_D=7 μM) that provides an approximately linear measure of Ca_{res}[37]. As such it is well suited to measuring the time course of presynaptic Ca_{res} (Fig. 2A) and detecting changes in Ca_{influx} during successive stimulations (Fig. 2B). However, with the bulk loading approach the size of the fluorescence change is proportional to the number of stimulated fibers, so the absolute Ca_{res} signal is not readily quantified with magnesium green. In contrast, fura-2 has a high affinity for

calcium[38,39] (K_D = 131 nM) so it provides a saturating sublinear response to increases in Ca_{res}[40–42]. This can be used to test for changes in the absolute size of Ca_{influx} because a change in the Ca_{influx} per stimulus would change the ratio between the fluorescence change produced by the first and second stimuli.

Immunohistochemistry

Two to four weeks after AAV injection, mice were anesthetized with ketamine and transcardially perfused with 4% PFA in PBS. The brain was removed and post-fixed for 24 hours. Slices (50 μm thick) were permeabilized (PBS + 0.4% Triton X-100) for 30 minutes and then prepared in blocking solution (PBS + 0.2% Triton X-100 + 2% normal goat serum [PBST]) for 30 min at room temperature. Slices were incubated overnight at 4°C in PBST with primary antibodies (anti-syt7 [Synaptic Systems, 105173], 1 μg/ml; 1:200, targeting AA 46–133 of syt7α, anti-vGlut1 [Synaptic Systems, 135304], 1 μg/ml; 1:500, and anti-calbindin-D28k [Sigma Aldrich, C9848], 1 μg/ml; 1:500), followed by incubation with secondary antibodies in PBST for 2 hr at room temperature. For both WT and syt7 KO mice, images from each brain region were acquired on a laser scanning confocal (Olympus, FluoView1200) using the same laser/microscope settings and processed in ImageJ identically.
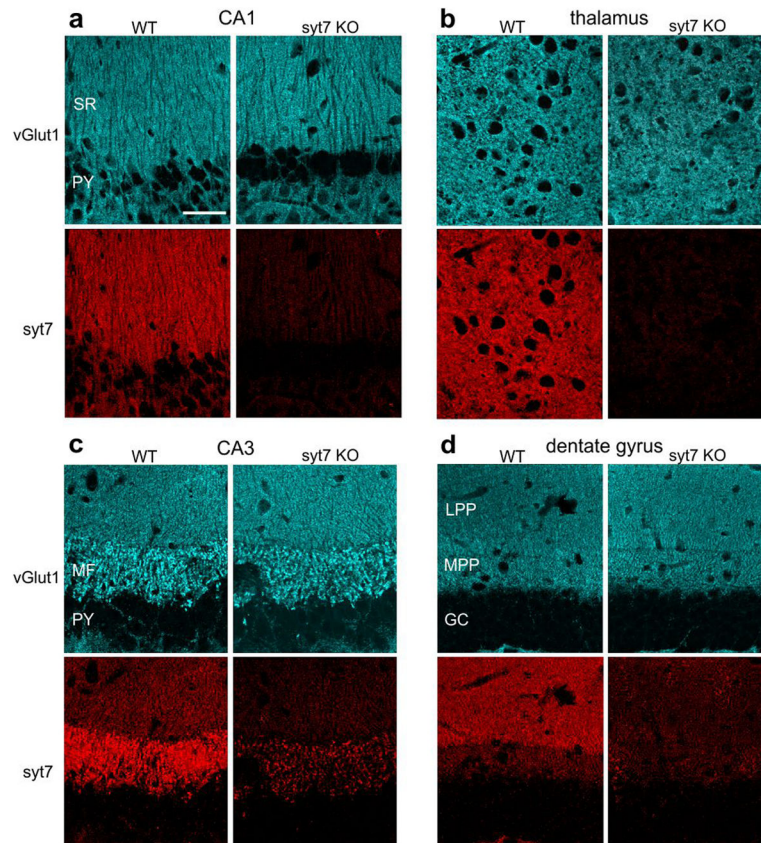
Extended Data
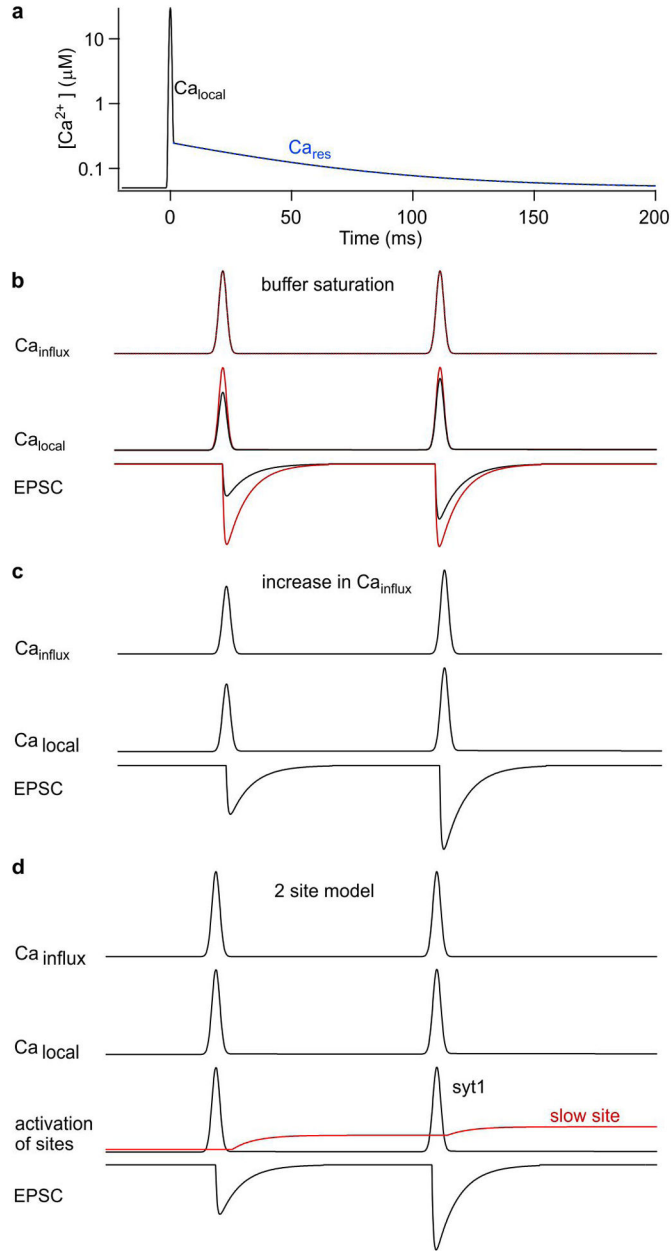
**Extended Data Figure 1. Possible mechanisms for synaptic facilitation**

It is established that calcium plays an important role in synaptic facilitation, and a number of mechanisms have been proposed that involve different aspects of calcium signaling[2]. Here we discuss the calcium signals that evoke rapid vesicle fusion, and also those thought to be involved in facilitation (**a**), and 3 mechanisms of facilitation are presented schematically[43] (**b–d**). **a**, To understand the mechanisms that have been proposed to account for facilitation, it is important to appreciate different aspects of presynaptic calcium signaling. Calcium signals are complex, but can be approximated by 2 components. An action potential opens calcium channels for less than a millisecond, and near open channels the calcium levels

reach tens of micromolar. Release sites near calcium channels experience high local calcium levels (Ca_{local}) that are highly dependent on the distance from open calcium channels. Ca_{local} can be reduced by high concentrations of fast calcium buffers that rapidly bind calcium. In addition there is a residual calcium signal (Ca_{res}) that results from calcium equilibrating within presynaptic terminals, before calcium is gradually removed over tens to hundreds of milliseconds. The amplitude of Ca_{res} (and also total influx of Ca^{2+}, Ca_{influx}) is determined by *all* of the calcium channels that open, not only those that produce Ca_{local} that drives release, and after initial equilibration Ca_{res} is roughly uniform throughout the presynaptic bouton. It is generally accepted that fast synaptic transmission is produced by calcium binding to syt1, syt2 or syt9 which have low-affinity binding sites, fast kinetics, and require the binding of multiple calcium ions[7,44]. The time course of release follows the time course of calcium channel opening, but with a brief delay (< 1 ms). Ca_{res} after a single stimulus is much smaller than Ca_{local}. Typical fluorescence-based approaches to measure calcium readily detect Ca_{res}, but are insensitive to Ca_{local} which is too localized and short-lived to measure. Note the y-axis is logarithmic to show both Ca_{local} and Ca_{res} in (**a**), but not in (**b–d**). **b**, For one mechanism of facilitation a fast calcium buffer is present in presynaptic terminals that binds calcium and reduces Ca_{local}. Stimulating twice in rapid succession results in the same calcium influx for both stimuli. If there is no fast presynaptic buffer, the amplitudes of Ca_{local} and the EPSCs are the same for both stimuli (red traces). If a fast high-affinity buffer is present (black traces), it reduces the initial Ca_{local} and reduces the amplitude of the initial EPSC, but if enough calcium enters and binds to the buffer, it reduces its ability to buffer calcium. As a result the second stimulus produces larger Ca_{local} than the first, and the EPSC is facilitated. **c**, A second possible mechanism is that more calcium enters for the second stimulus, and as a result there is more neurotransmitter release. This could arise from a spike broadening, or from the modulation of calcium channels. It is possible that influx through all calcium channels in the presynaptic terminal would be increased, in which case both Ca_{res} and Ca_{local} would be increased. It is also possible that the only calcium channels that are modulated are the subset that produce Ca_{local} that triggers release, in which case Ca_{res} would not be significantly increased. **d**, Finally, it is possible that there is a specialized calcium sensor that produces facilitation that is distinct from syt1[2,4,45]. Previous studies have shown that such a sensor would need to be sensitive to Ca_{res} based on the observation that facilitation is altered at some synapses by manipulations that affect Ca_{res} without affecting Ca_{local}. According to this scheme, release is mediated by syt1 but calcium binding to a second sensor would increase *p*. The sensor is sufficiently slow that it does not influence release evoked by the first stimulus, but it able to influence release evoked by a second stimulus.

Extended Data Figure 2. Immunohistochemistry of syt7 expression at 4 different synapses
Fluorescent images of immunostaining for vGlut1 (top) and syt7 (bottom) in slices from WT
and syt7 KO animals, showing (**a**) the stratum radiatum (SR) of hippocampal CA1 region,
(**b**) the ventral thalamus, (**c**) mossy fibers (MF) in hippocampal CA3, and (**d**) the lateral and
medial performant paths (LPP and MPP) in the outer molecular layer of the dentate gyrus.
Notably, syt7 expression in WT animals was higher in the LPP, where synapses exhibit
facilitation, compared to the MPP, where synapses exhibit depression. Scale bar, 50 μm. The
presence of syt7 labeling in regions containing CA3→CA1 synapses, layer 6 to thalamus
synapses, MF synapses and LPP→granule cell synapses that are also colabeled with
antibodies to the presynaptic marker for glutamatergic synapses vGlut1, suggests that syt7 is
located presynaptically at these synapses. It is, however, difficult to obtain sufficient
resolution with confocal microscopy in brain slices to unambiguously establish that syt7 is
located presynaptically at these synapses. Importantly, the Allen Brain atlas suggests that the
presynaptic cells for these synapses contain mRNA for syt7[46]. Lastly, immunoelectron
microscopy revealed selective staining of presynaptic boutons in the CA1 region of the
hippocampus[16].
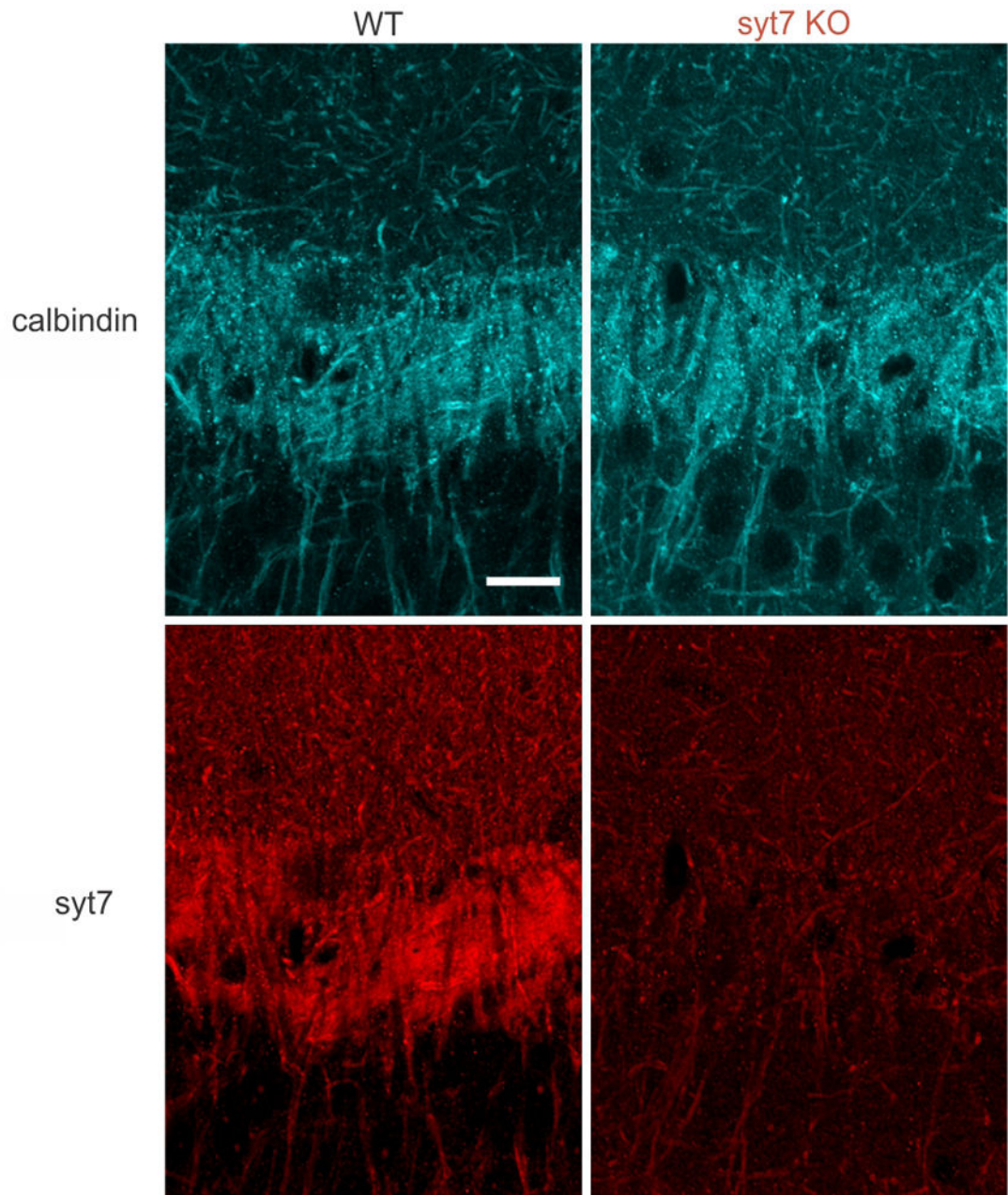
**Extended Data Figure 3. Immunohistochemistry of syt7 and calbindin expression at mossy fiber synapses**

Fluorescent images of immunostaining for calbindin-D28k, which predominantly labels mossy fibers in the CA3 region of the hippocampus[9,47] (top) and syt7 (bottom) in slices from WT and syt7 KO animals. Colocalization of syt7 and calbindin staining in WT animals provides further support for the expression of syt7 in mossy fiber terminals. Scale bar, 20 μm.
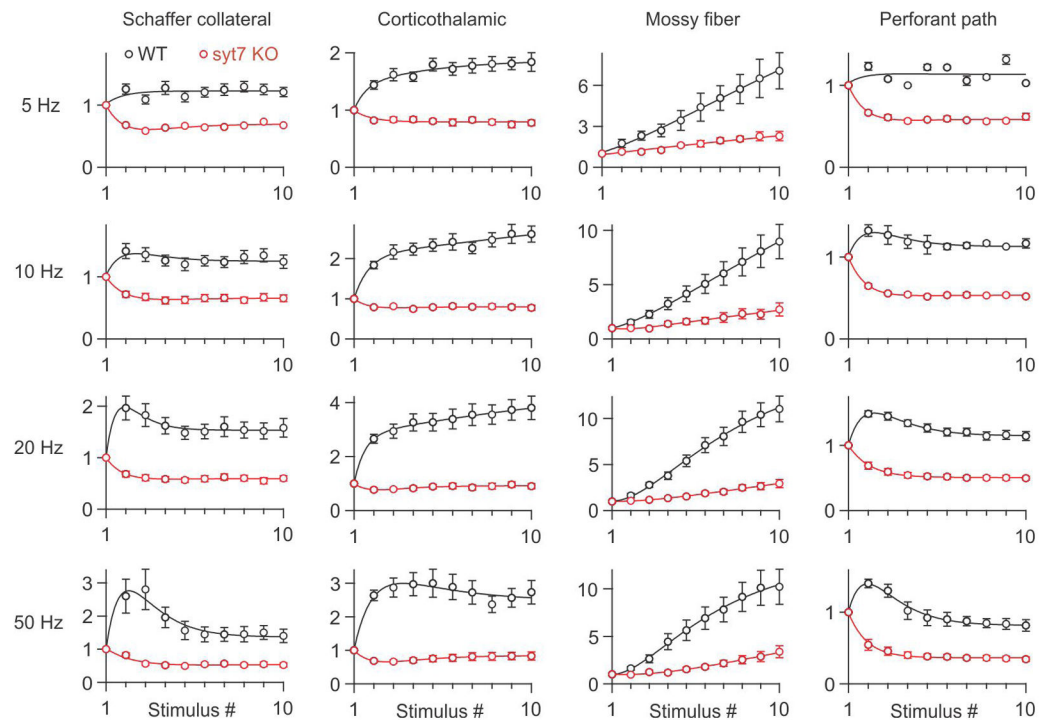
Extended Data Figure 4. Loss of facilitation in syt7 KO animals at multiple frequencies
Average normalized synaptic responses evoked by extracellular stimulation with trains at
frequencies from 5–50 Hz at four synapses in slices from WT and syt7 KO animals.
Enhancement during trains was eliminated for all synapses other than mossy fiber synapses,
where significant enhancement was present by the 5th stimulus for 5 Hz and 10 Hz, the 3rd
stimulus for 20 Hz and the 6th stimulus for 50 Hz (compared to 1 by a Wilcoxon signed
rank test, $P < 0.05$). This indicates that another form of synaptic enhancement gradually
builds during repetitive activation and is consistent with a specialized form of synaptic
enhancement that has been described at mossy fiber synapses in which spike broadening
gradually builds during repetitive activation and leads to increased calcium influx. The
numbers of experiments are shown in Extended Data Table 1.
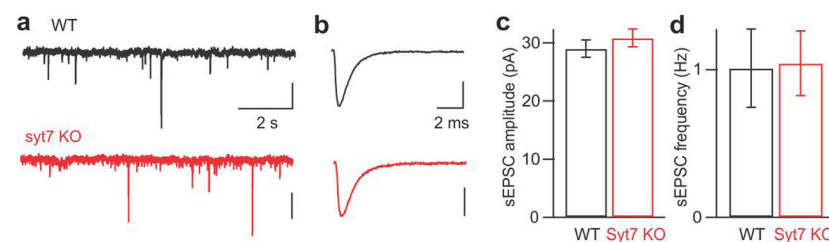
**Extended Data Figure 5. Spontaneous release is similar in WT and syt7 KO animals**
a, Representative sEPSCs recorded from voltage-clamped hippocampal CA1 cells in WT
(black) and KO (red) animals. Vertical scale bars, 20 pA. **b**, Representative sEPSCs,
averaged from >50 events recorded in WT and KO animals. Vertical scale bars, 10 pA. **c–d**,

Average sEPSC (**c**) amplitude and (**d**) frequency in WT (N = 16) and syt7 KO animals (N = 18).
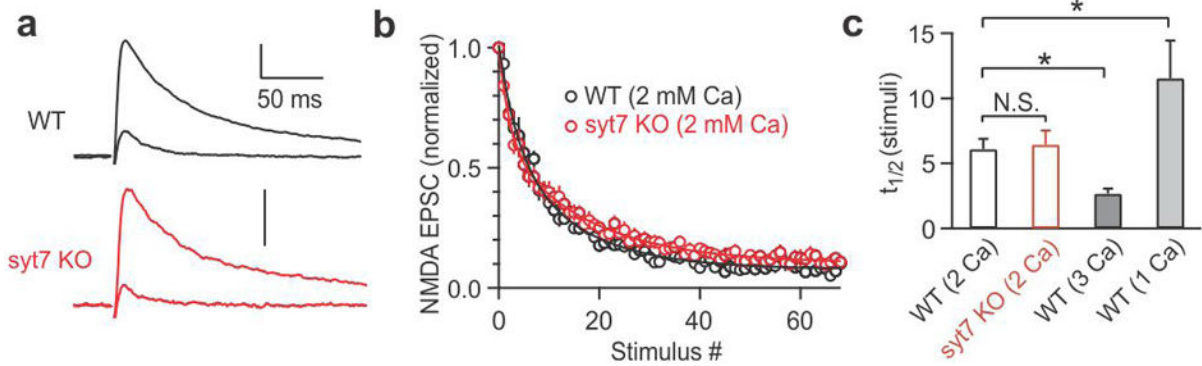

Extended Data Figure 6. MK801 blockade of NMDA receptor-mediated EPSCs reveals similar initial release probability in WT and KO synapses

a, Representative NMDA-EPSCs recorded in WT and KO animals before the application of MK801 (average of 10 traces) and after stimulation in the presence of MK801 (average response of 15–20th stimuli). Vertical scale bars, 100 pA. **b**, Average NMDA-EPSCs recorded in the presence of MK801, normalized to the first stimulus. **c**, Half-decay times of NMDA-EPSC amplitudes. *$P < 0.05$, one-way ANOVA with Tukey's post hoc test. N.S., not significant. The number of experiments is shown in Extended Data Table 2.
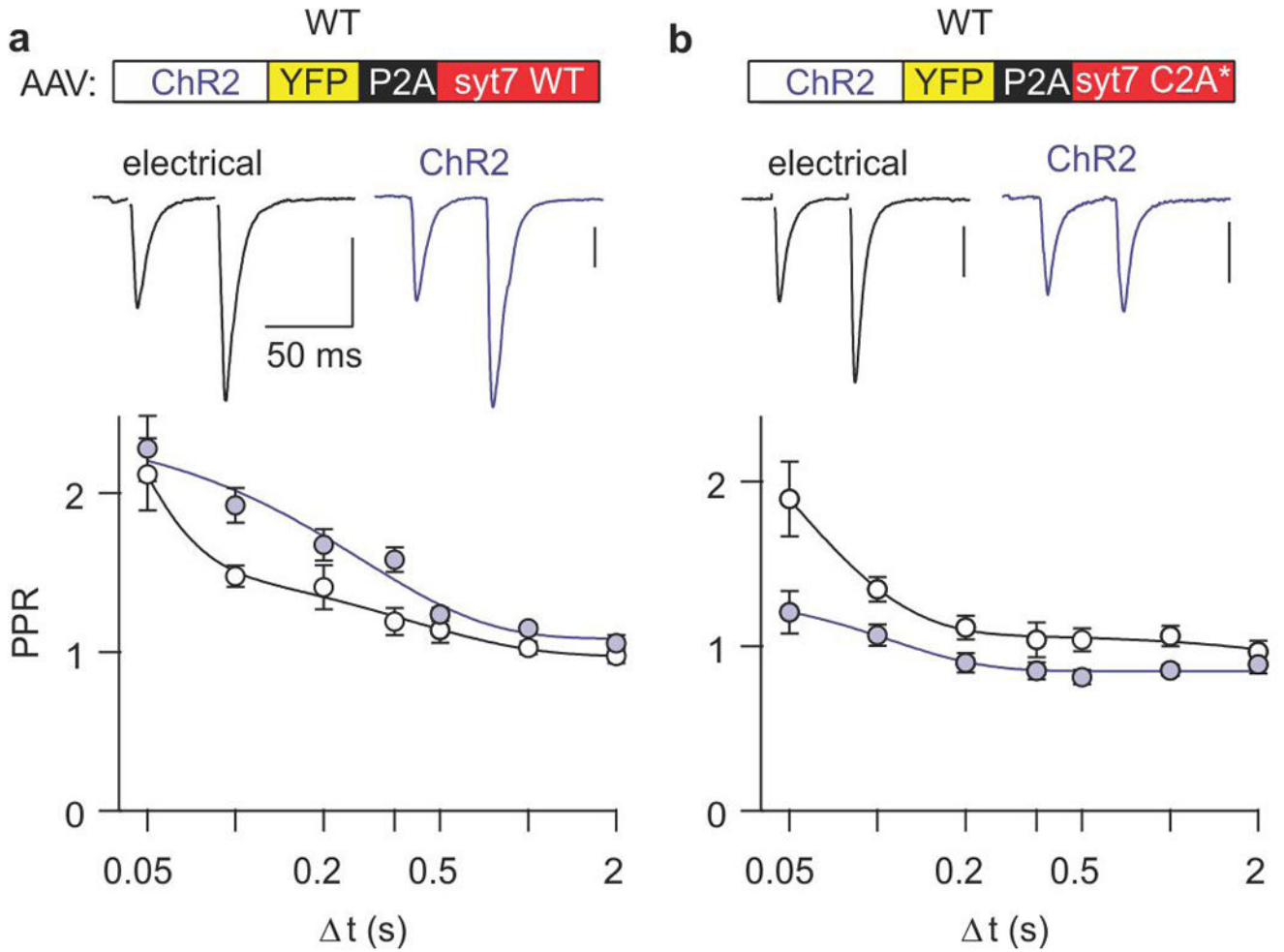
Extended Data Figure 7. Effect of virally-expressed syt7 WT and syt7 C2A* in WT animals
a–b, (Top) AAV was injected into the hippocampal CA3 region in WT animals to express ChR2 and (**a**) syt7 WT or (**b**) syt7 C2A*. (Bottom) Representative EPSCs and average paired-pulse ratios for responses evoked electrically and optically in WT slices with AAV-driven expression of (a) syt7 WT (electrical, N = 12; optical, N = 13) and (b) syt7 C2A* (electrical, N = 5; optical, N = 13). Vertical scale bars, 100 pA.
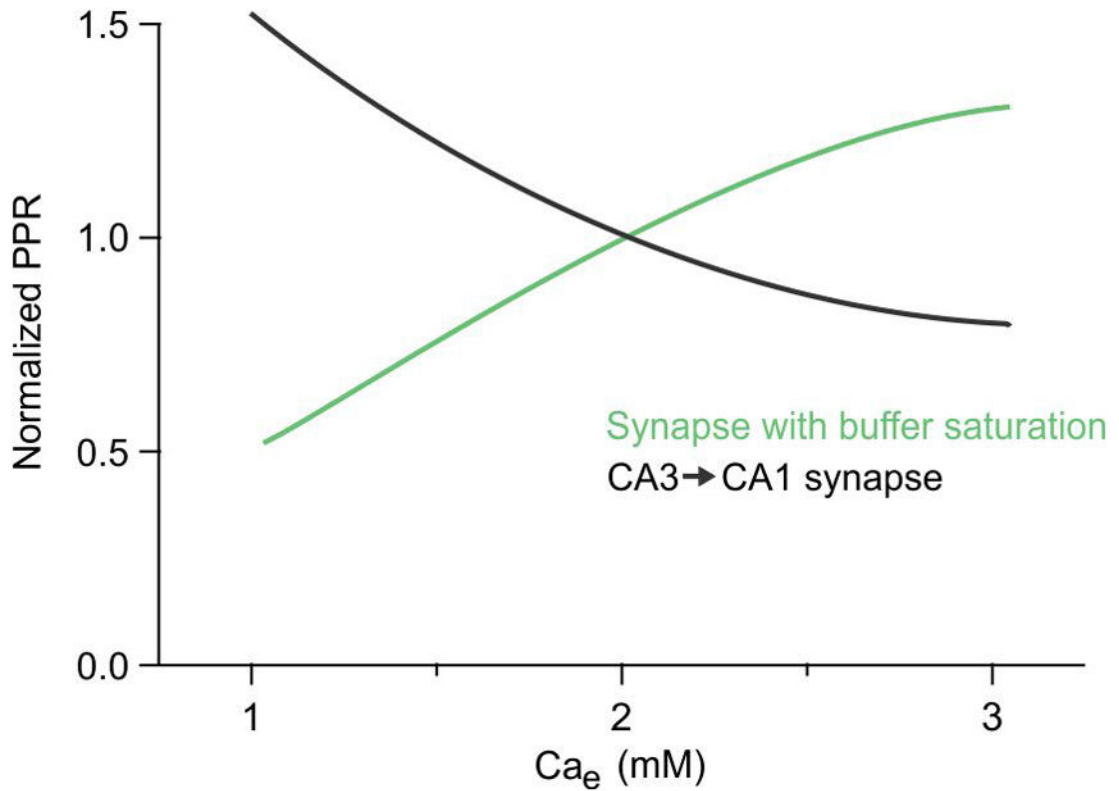
Extended Data Figure 8. Evidence suggests that syt7 does not produce facilitation by acting as a local calcium buffer at the CA3→CA1 synapse

This graph illustrates the general relationship between PPR and external calcium for synapses in which buffer saturation produces facilitation (green) and for facilitation observed at the CA3→CA1 synapse and many other synapses (black)[9]. It has been shown previously that the for buffer saturation mechanism (Extended Data Fig. 1B) the amplitude of facilitation is reduced when Ca_{influx} is reduced by lowering external calcium[9]. This can be understood by considering that this form of facilitation is thought to require sufficient Ca_{influx} to saturate the endogenous buffer, and thereby reduce its ability to buffer calcium for subsequent stimuli. If Ca_{influx} is low then there is insufficient calcium entry to bind very much of the endogenous buffer, and little facilitation would result. In addition, as shown in Extended Data Figure 1 for a calcium buffer to produce facilitation it would need to buffer calcium sufficiently that it would reduce initial *p*. We have shown, however, that *p* is unaltered in syt7 knockouts. This is perhaps not surprising in light of the fact that syt7 is thought to be located on the plasma membrane, and in cases where this type of facilitation has been observed it is associated with high concentrations of a fast cytosolic buffer[9].

Extended Data Table 1

Number of electrophysiological recordings from WT and syt7 KO animals.

Figure	Synapse	Experiment	Genotype	# of Recordings	# of Animals
Figure 1a	Schaffer collateral	Paired-pulse	WT	13	6

Figure	Synapse	Experiment	Genotype	# of Recordings	# of Animals
			KO	17	5
Figure 1b	Corticothalamic	Paired-pulse	WT	23	8
			KO	23	5
Figure 1c	Hippocampal mossy fiber	Paired-pulse	WT	10	6
			KO	8	4
Figure 1d	Lateral perforant path	Paired-pulse	WT	6	3
			KO	13	3
Figure 1e, Extended Data Figure 4	Schaffer collateral	Trains (2–50 Hz)	WT	14	6
		Trains (2–50 Hz)	KO	17	5
Figure 1f, Extended Data Figure 4	Corticothalamic	Trains (2–50 Hz)	WT	16	8
		Train (2 Hz)	KO	5	2
		Trains (5–50 Hz)	KO	12	3
Figure 1g, Extended Data Figure 4	Hippocampal mossy fiber	Train (2 Hz)	WT	3	2
		Train (5 Hz)	WT	7	4
		Train (10–50 Hz)	WT	10	5
		Train (2–5 Hz)	KO	3	2
		Train (10–50 Hz)	KO	8	4
Figure 1h, Extended Data Figure 4	Lateral perforant path	Train (2–10 Hz)	WT	3	2
		Train (20–50 Hz)	WT	6	3
		Train (2–5 Hz)	KO	5	2
		Train (10 Hz)	KO	10	3
		Train (20–50 Hz)	KO	13	3

Extended Data Table 2

Number of experiments related to the Ca^{2+}-dependence of probability of release.

Figure	Experiment	Condition	Genotype	# of Recordings	# of Animals
Figure 2a,b	Presynaptic Ca^{2+} imaging	Magnesium Green	WT	11	2
			KO	10	2
Figure 2c	Presynaptic Ca^{2+} imaging	Fura-2	WT	14	3
			KO	10	2
Figure 2d–f	Ca^{2+}-dependence of CA3-CA1 EPSC	0.5 mM Ca	WT	12	5
		1 mM Ca	WT	9	4
		2 mM Ca *	WT	15	6
		3 mM Ca	WT	6	2
		0.5 mM Ca	KO	8	4
		1 mM Ca	KO	7	6
		2 mM Ca *	KO	10	8
		3 mM Ca	KO	4	2
Figure 3a,b	fEPSP vs. fiber volley	20–100 uA stimulation	WT	44	11
			KO	25	8

Figure	Experiment	Condition	Genotype	# of Recordings	# of Animals
Figure 3c,d	Ca^{2+}-dependence of CA3-CA1 fEPSP	0.5 mM Ca	WT	4	2
		1 mM Ca	WT	11	5
		2 mM Ca *	WT	11	5
		3 mM Ca	WT	8	3
		0.5 mM Ca	KO	4	4
		1 mM Ca	KO	8	4
		2 mM Ca *	KO	9	5
		3 mM Ca	KO	6	3
Figure 3e–g	MK801 blockade of NMDAR fEPSP	2 mM Ca, single stim	WT	6	2
		2 mM Ca, tripple stim	WT	5	3
		2 mM Ca, single stim	KO	6	3
		2 mM Ca, tripple stim	KO	4	3
Extended Data Figure 6	MK801 blockade of NMDAR EPSC	1 mM Ca	WT	14	3
		2 mM Ca	WT	11	4
		3 mM Ca	WT	3	2
		2 mM Ca	KO	9	4

*
To normalize responses in different Ca^{2+} concentrations, all Ca^{2+}-dependence experiments included recordings in 2 mM Ca^{2+} followed by wash in of different Ca^{2+} concentrations.

Acknowledgments

References

1. Feng TP. Studies on the neuromuscular junction. XVIII The local potentials around n-m junctions induced by single and multiple volleys. Chin J Physiol. 1940; 15:367–404.

2. Zucker RS, Regehr WG. Short-term synaptic plasticity. Annu Rev Physiol. 2002; 64:355–405.10.1146/annurev.physiol.64.092501.114547 [PubMed: 11826273]

3. Abbott LF, Regehr WG. Synaptic computation. Nature. 2004; 431:796–803.10.1038/nature03010 [PubMed: 15483601]

4. Atluri PP, Regehr WG. Determinants of the time course of facilitation at the granule cell to Purkinje cell synapse. J Neurosci. 1996; 16:5661–5671. [PubMed: 8795622]

5. Bertram R, Sherman A, Stanley EF. Single-domain/bound calcium hypothesis of transmitter release and facilitation. J Neurophysiol. 1996; 75:1919–1931. [PubMed: 8734591]

6. Felmy F, Neher E, Schneggenburger R. Probing the intracellular calcium sensitivity of transmitter release during synaptic facilitation. Neuron. 2003; 37:801–811.10.1016/s0896-6273(03)00085-0 [PubMed: 12628170]

7. Sudhof TC. A molecular machine for neurotransmitter release: synaptotagmin and beyond. Nat Med. 2013; 19:1227–1231.10.1038/nm.3338 [PubMed: 24100992]

8. Matveev V, Zucker RS, Sherman A. Facilitation through buffer saturation: Constraints on endogenous buffering properties. Biophys J. 2004; 86:2691–2709.10.1016/s0006-3495(04)74324-6 [PubMed: 15111389]

9. Blatow M, Caputi A, Burnashev N, Monyer H, Rozov A. Ca2+ buffer saturation underlies paired pulse facilitation in calbindin-D28k-containing terminals. Neuron. 2003; 38:79–88.10.1016/s0896-6273(03)00196-x [PubMed: 12691666]

10. Mochida S, Few AP, Scheuer T, Catterall WA. Regulation of presynaptic Ca(V)2.1 channels by Ca2+ sensor proteins mediates short-term synaptic plasticity. Neuron. 2008; 57:210–216.10.1016/j.neuron.2007.11.036 [PubMed: 18215619]

11. Sippy T, Cruz-Martin A, Jeromin A, Schweizer FE. Acute changes in short-term plasticity at synapses with elevated levels of neuronal calcium sensor-1. Nat Neurosci. 2003; 6:1031–1038.10.1038/nn1117 [PubMed: 12947410]

12. Tsujimoto T, Jeromin A, Saitoh N, Roder JC, Takahashi T. Neuronal calcium sensor 1 and activity-dependent facilitation of P/Q-type calcium currents at presynaptic nerve terminals. Science. 2002; 295:2276–2279.10.1126/science.1068278 [PubMed: 11910115]

13. Muller M, Felmy F, Schneggenburger R. A limited contribution of Ca2+ current facilitation to paired-pulse facilitation of transmitter release at the rat calyx of Held. J Physiol. 2008; 586:5503–5520.10.1113/jphysiol.2008.155838 [PubMed: 18832426]

14. Hui E, et al. Three distinct kinetic groupings of the synaptotagmin family: candidate sensors for rapid and delayed exocytosis. Proc Natl Acad Sci U S A. 2005; 102:5210–5214.10.1073/pnas.0500941102 [PubMed: 15793006]

15. Li C, et al. Ca2+-dependent and -independent activities of neural and non-neural synaptotagmins. Nature. 1995; 375:594–599.10.1038/375594a0 [PubMed: 7791877]

16. Sugita S, et al. Synaptotagmin VII as a plasma membrane Ca2+ sensor in exocytosis. Neuron. 2001; 30:459–473. [PubMed: 11395007]

17. Wen H, et al. Distinct roles for two synaptotagmin isoforms in synchronous and asynchronous transmitter release at zebrafish neuromuscular junction. Proc Natl Acad Sci U S A. 2010; 107:13906–13911.10.1073/pnas.1008598107 [PubMed: 20643933]

18. Bacaj T, et al. Synaptotagmin-1 and synaptotagmin-7 trigger synchronous and asynchronous phases of neurotransmitter release. Neuron. 2013; 80:947–959.10.1016/j.neuron.2013.10.026 [PubMed: 24267651]

19. Liu H, et al. Synaptotagmin 7 functions as a Ca2+-sensor for synaptic vesicle replenishment. eLife. 2014; 3:e01524.10.7554/eLife.01524 [PubMed: 24569478]

20. Descheenes M, Hu B. Electrophysiology and Pharmacology of the Corticothalamic Input to Lateral Thalamic Nuclei: an Intracellular Study in the Cat. Eur J Neurosci. 1990; 2:140–152. [PubMed: 12106057]

21. Lomo T. Potentiation of monosynaptic EPSPs in the perforant path-dentate granule cell synapse. Exp Brain Res. 1971; 12:46–63. [PubMed: 5543201]

22. Geiger JR, Jonas P. Dynamic control of presynaptic Ca2+ inflow by fast-inactivating K+ channels in hippocampal mossy fiber boutons. Neuron. 2000; 28:927–939. [PubMed: 11163277]

23. Geppert M, et al. Synaptotagmin I: a major Ca2+ sensor for transmitter release at a central synapse. Cell. 1994; 79:717–727. [PubMed: 7954835]

24. Dingledine R, Somjen G. Calcium dependence of synaptic transmission in the hippocampal slice. Brain Res. 1981; 207:218–222.10.1016/0006-8993(81)90697-1 [PubMed: 6258732]

25. Manabe T, Nicoll RA. Long-term potentiation: evidence against an increase in transmitter release probability in the CA1 region of the hippocampus. Science. 1994; 265:1888–1892. [PubMed: 7916483]

26. Gustavsson N, et al. Impaired insulin secretion and glucose intolerance in synaptotagmin-7 null mutant mice. Proc Natl Acad Sci U S A. 2008; 105:3992–3997.10.1073/pnas.0711700105 [PubMed: 18308938]

27. Martinez I, et al. Synaptotagmin VII regulates Ca2+-dependent exocytosis of lysosomes in fibroblasts. J Cell Biol. 2000; 148:1141–1149. [PubMed: 10725327]

28. Klyachko VA, Stevens CF. Excitatory and feed-forward inhibitory hippocampal synapses work synergistically as an adaptive filter of natural spike trains. PLoS Biol. 2006; 4:e207.10.1371/journal.pbio.0040207 [PubMed: 16774451]

29. MacLeod KM, Horiuchi TK, Carr CE. A role for short-term synaptic facilitation and depression in the processing of intensity information in the auditory brain stem. J Neurophysiol. 2007; 97:2863–2874.10.1152/jn.01030.2006 [PubMed: 17251365]

30. Mongillo G, Barak O, Tsodyks M. Synaptic theory of working memory. Science. 2008; 319:1543–1546.10.1126/science.1150769 [PubMed: 18339943]

31. Chakrabarti S, et al. Impaired membrane resealing and autoimmune myositis in synaptotagmin VII-deficient mice. J Cell Biol. 2003; 162:543–549.10.1083/jcb.200305131 [PubMed: 12925704]

32. Kim JH, et al. High cleavage efficiency of a 2A peptide derived from porcine teschovirus-1 in human cell lines, zebrafish and mice. PLoS One. 2011; 6:e18556.10.1371/journal.pone.0018556 [PubMed: 21602908]

33. Zolotukhin S, et al. Recombinant adeno-associated virus purification using novel methods improves infectious titer and yield. Gene Ther. 1999; 6:973–985.10.1038/sj.gt.3300938 [PubMed: 10455399]

34. Jackman SL, Beneduce BM, Drew IR, Regehr WG. Achieving high-frequency optical control of synaptic transmission. J Neurosci. 2014; 34:7704–7714.10.1523/JNEUROSCI.4694-13.2014 [PubMed: 24872574]

35. Kamiya H, Shinozaki H, Yamamoto C. Activation of metabotropic glutamate receptor type 2/3 suppresses transmission at rat hippocampal mossy fibre synapses. J Physiol. 1996; 493(Pt 2):447–455. [PubMed: 8782108]

36. Zhao M, Hollingworth S, Baylor SM. Properties of tri- and tetracarboxylate Ca2+ indicators in frog skeletal muscle fibers. Biophys J. 1996; 70:896–916.10.1016/S0006-3495(96)79633-9 [PubMed: 8789107]

37. Kreitzer AC, Regehr WG. Modulation of transmission during trains at a cerebellar synapse. J Neurosci. 2000; 20:1348–1357. [PubMed: 10662825]

38. Brenowitz SD, Regehr WG. Calcium dependence of retrograde inhibition by endocannabinoids at synapses onto Purkinje cells. J Neurosci. 2003; 23:6373–6384. [PubMed: 12867523]

39. Grynkiewicz G, Poenie M, Tsien RY. A new generation of Ca2+ indicators with greatly improved fluorescence properties. J Biol Chem. 1985; 260:3440–3450. [PubMed: 3838314]

40. Sabatini BL, Regehr WG. Detecting changes in calcium influx which contribute to synaptic modulation in mammalian brain slice. Neuropharmacology. 1995; 34:1453–1467. [PubMed: 8606793]

41. Maravall M, Mainen ZF, Sabatini BL, Svoboda K. Estimating intracellular calcium concentrations and buffering without wavelength ratioing. Biophys J. 2000; 78:2655–2667.10.1016/S0006-3495(00)76809-3 [PubMed: 10777761]

42. Sabatini BL, Svoboda K. Analysis of calcium channels in single spines using optical fluctuation analysis. Nature. 2000; 408:589–593.10.1038/35046076 [PubMed: 11117746]

43. Regehr WG. Short-term presynaptic plasticity. Cold Spring Harbor perspectives in biology. 2012; 4:a005702.10.1101/cshperspect.a005702 [PubMed: 22751149]

44. Kaeser PS, Regehr WG. Molecular mechanisms for synchronous, asynchronous, and spontaneous neurotransmitter release. Annu Rev Physiol. 2014; 76:333–363.10.1146/annurev-physiol-021113-170338 [PubMed: 24274737]

45. Kamiya H, Zucker RS. Residual Ca2+ and short-term synaptic plasticity. Nature. 1994; 371:603–606.10.1038/371603a0 [PubMed: 7935792]

46. Website:© *2015 Allen Institute for Brain Science. Allen Brain Atlas [Internet]. Available from:* http://www.brain-map.org.

47. Celio MR. Calbindin D-28k and parvalbumin in the rat nervous system. Neuroscience. 1990; 35:375–475. [PubMed: 2199841]
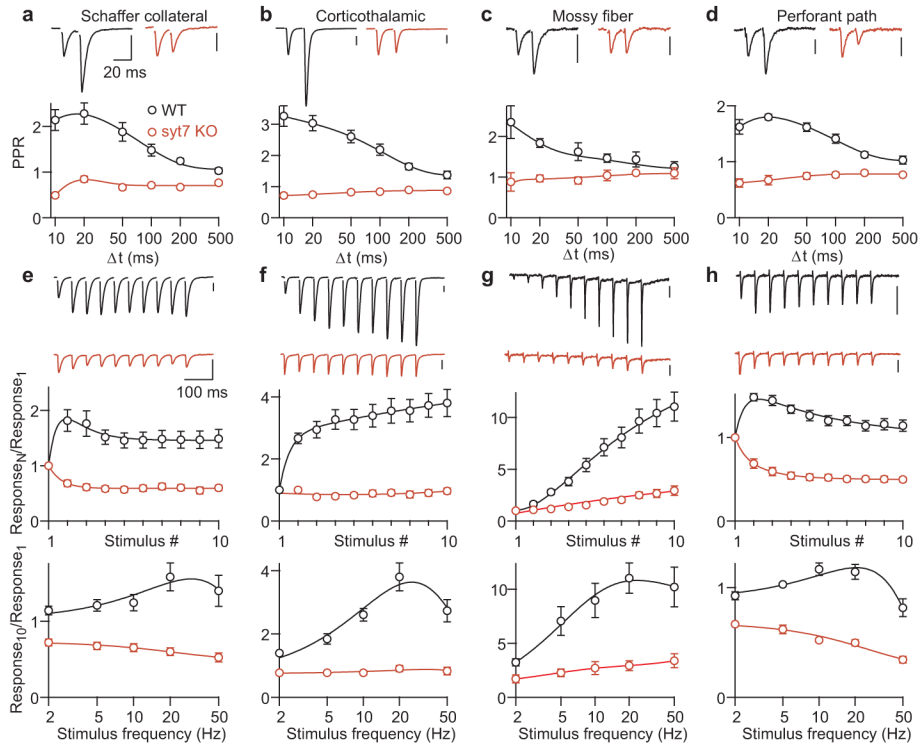
Figure 1. Facilitation is absent in syt7 KO mice

a–d, Representative traces (top) and average paired-pulse ratios (PPR) at different interstimulus intervals (Δt) (bottom) recorded in slices prepared from WT (black) and syt7 KO animals (red). Postsynaptic responses were recorded using whole-cell voltage clamp from (**a**) hippocampal CA1 pyramidal cells, and (**b**) thalamic relay cells. fEPSPs were recorded from (**c**) hippocampal-mossy-fiber to CA3 synapses, and (**d**) lateral-performant-path synapses in the dentate gyrus. Vertical scale bars, 100 pA (**a,b**) and 100 μV (**c,d**). **e–h**, Synaptic responses to 20 Hz trains from the same preparations as **a–d** (top), normalized amplitudes during 20 Hz trains (middle), and normalized responses to the 10th stimulus as a function of stimulus frequency (bottom). Peak PPR was significantly different for WT and syt7 KO mice at all synapses, as was response$_{10}$/response$_1$ for 5 to 50 Hz trains ($P < 0.01$, Student's t-test). Data in this and subsequent figures represent mean ± SEM. Number of experiments shown in Extended Data Table 1.
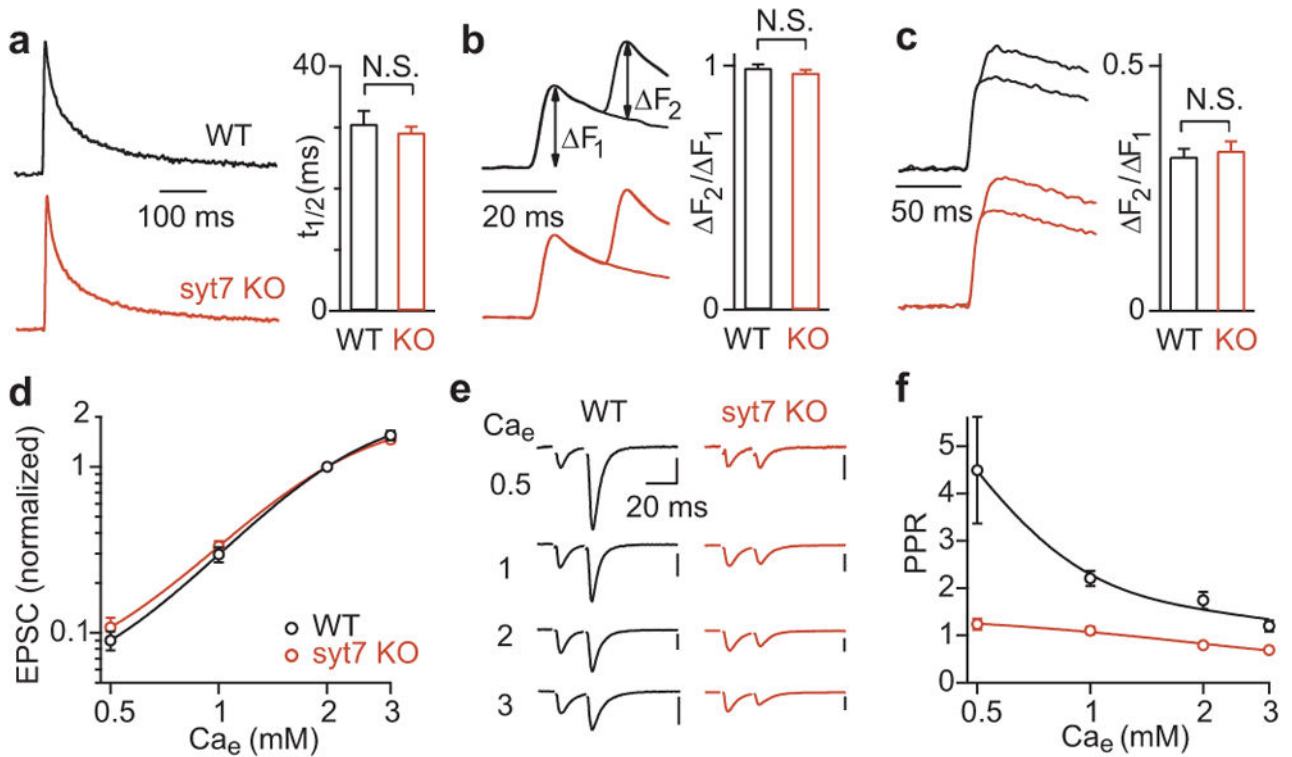
Figure 2. Facilitation is altered in syt7 KO animals despite similar presynaptic Ca^{2+} signals

a, Presynaptic Ca$_{res}$ evoked by a single stimulus recorded from Schaffer collateral fibers loaded with a low-affinity Ca^{2+} indicator (left), and Ca$_{res}$ half-decay times (right). N.S., not significant. **b**, Ca$_{res}$ signals recorded with low-affinity indicator evoked by 1 or 2 stimuli (left). The ratio of the increase in Ca$_{res}$ evoked by the first (ΔF_1) and second (ΔF_2) stimuli (right). **c**, Ca$_{res}$ signals recorded with high-affinity indicator evoked by 1 or 2 stimuli. **d**, Average EPSC amplitudes for CA3→CA1 synapses recorded in different external Ca^{2+} (Ca$_e$) concentrations, normalized to the amplitude in 2 mM Ca$_e$. **e**, EPSCs recorded in different Ca$_e$. Vertical scale bars, 50, 100, 200 and 300 pA in 0.5, 1, 2 and 3 mM Ca$_e$ respectively. **f**, PPR for interstimulus interval of 20 ms recorded in different Ca$_e$. In 0.5 mM Ca^{2+} PPR in KOs (1.24 ± 0.12) was not significantly different from 1 ($P = 0.084$, Wilcoxon signed rank test). Number of experiments is shown in Extended Data Table 2.
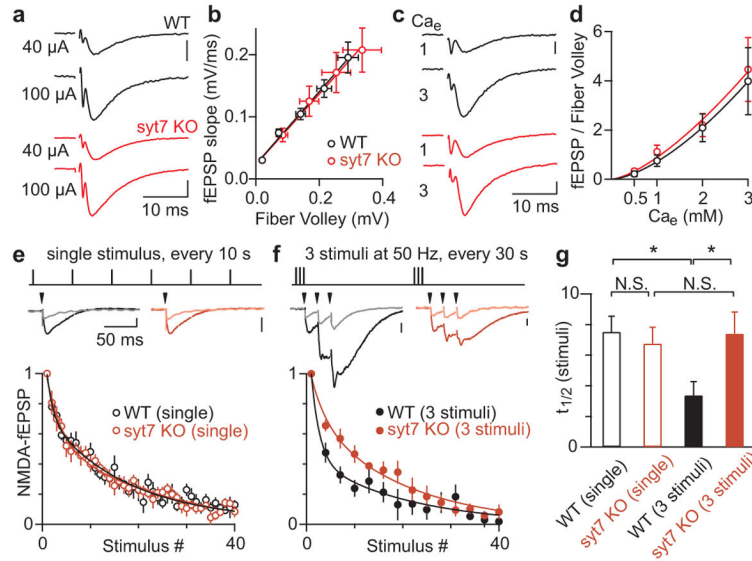
Figure 3. Change in the initial probability of release does not underlie the absence of facilitation in syt7 KO mice

a, Extracellular recordings of presynaptic fiber volley and fEPSP evoked by the indicated stimulus intensities. Scale bar, 200 µV. **b**, fEPSP slope plotted against fiber volley amplitude, for 20–100 µA stimulation. **c**, fEPSPs recorded in 1 and 3 mM Ca_e. Scale bar, 100 µV. **d**, Average ratio of the fEPSP to the fiber volley in different Ca_e. **e**, (Top) Initial release probability was measured by stimulating Schaffer collaterals every 10 seconds while recording NMDA-fEPSPs before and after MK801 bath application. (Middle) Traces averaged from 10 trials before (dark traces), and trials 10–15 after MK801 application (light traces). (Bottom) Average NMDA-fEPSPs amplitudes evoked in the presence of MK801. **f**, Same as in (e) but with 3 stimuli at 50 Hz every 30 seconds. First response to trains is shown. **g**, Half-decay times of NMDA-fEPSP amplitudes in the presence of MK801. *$P <$ 0.05, one-way ANOVA with Tukey's post hoc test. N.S., not significant. Number of experiments shown in Extended Data Table 2.
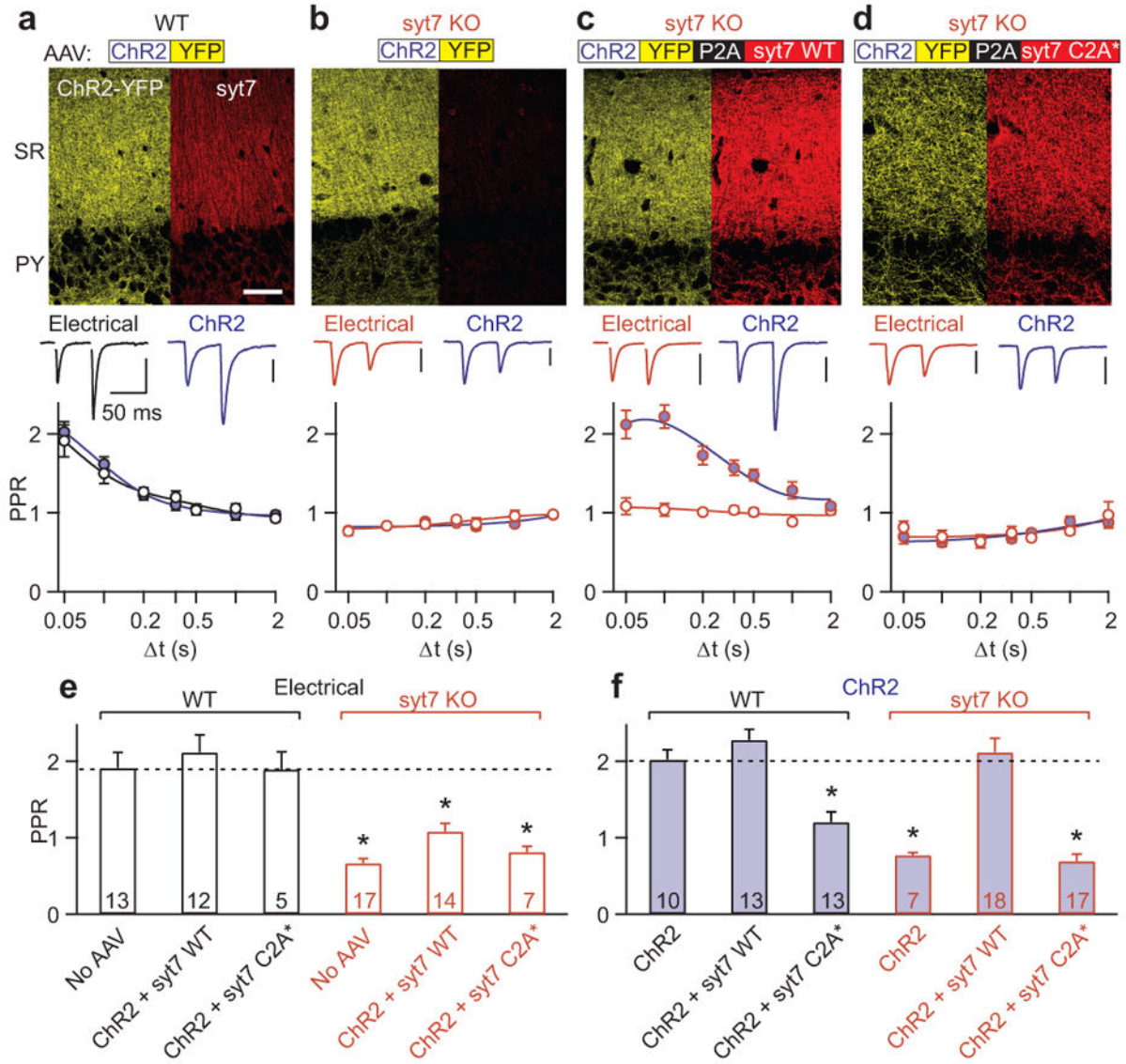
Figure 4. Viral expression of syt7 restores facilitation at Schaffer collateral synapses
a–d, (Top) Fluorescence images of ChR2-YFP and syt7 immunostaining in the CA1 region after AAV injection into CA3 to express the indicated proteins in WT animals (**a**) or syt7 KO animals (**b–d**). Stratum pyramidale (PY) and stratum radiatum (SR). Scale bar, 100 μm. (Bottom) EPSCs and PPRs for responses evoked electrically (open symbols) and optically (blue symbols). In **a** and **b** only ChR2-YFP was expressed, in **c** both ChR2-YFP and syt7(WT) were expressed (separated by a P2A cleavage peptide) and in **d** ChR2-YFP and Ca^{2+}-insensitive syt7C2A* were expressed. **e–f**, Summary of PPRs for 50 ms interstimulus interval. Asterisks denote significant difference from responses evoked electrically in uninjected WT animals (**e**), or optically in WT animals expressing ChR2 alone (**f**). *$P <$ 0.05, one-way ANOVA with Tukey's post hoc test. Number of experiments shown on bar graphs.